

A Soft X-Ray Grating Monochromator for Undulator Radiation

R. Reininger, V. Saile

Hamburger Synchrotronstrahlungslabor HASYLAB at DESY, Hamburg

ISSN 0723-7979

DESY behält sich alle Rechte für den Fall der Schutzrechtserteilung und für die wirtschaftliche Verwertung der in diesem Bericht enthaltenen Informationen vor.

DESY reserves all rights for commercial use of information included in this report, especially in case of filing application for or grant of patents.

To be sure that your preprints are promptly included in the
HIGH ENERGY PHYSICS INDEX ,
send them to the following address (if possible by air mail) :

DESY
Bibliothek
Notkestrasse 85
2 Hamburg 52
Germany

INTRODUCTION

From the performance of several high resolution soft-x-ray monochromators it became clear that slope errors in the aspherical optical elements enclosed by the slits deteriorate significantly the energy resolution. The SX-700/1 [1-3] achieved source size limited resolution only after a new focusing elliptical mirror with slope errors less than ± 0.9 arcsec (the minimum achieved with the present aspherical technology) was available [4]. The same type of monochromator accepting the radiation from another bending magnet at the BESSY storage ring, at which the source size is smaller, showed an improved energy resolution. However, this was obtained on the expense of intensity by shadowing off the elliptical mirror to 1% of its optical surface [5].

The highest resolving power in the soft-x ray range has been recently obtained [6] with the DRAGON monochromator designed by C.T. Chen [7]. The instrument is based on spherical elements and equipped with a movable exit slit (4.0-4.7 m). Its main disadvantages are, however, its yet low throughput and the varying exit arm length. An additional point to be taken into account when considering the possibility of matching such a monochromator to a powerful undulator [8] beam-line as the one under consideration is the severe heat load to which the narrow entrance slit (10 μm) will be exposed. This argument guided us to choose a monochromator without an entrance slit, discarding a DRAGON type monochromator for our new XUV beamline.

The perfect matching between the acceptance of a plane grating monochromator as the FLIPPER, to the undulator beam line W1 at HASYLAB [9] convinced us to search for an instrument based on a plane grating monochromator for the new XUV undulator.

We present below a modification of the SX-700 optical design in which the elliptical focusing mirror is replaced by a spherical one. The aberration resolution limit introduced by a spherical mirror can be made smaller than the resolution limit due to the source size by an appropriate extension of the exit slit arm. An optimization procedure was performed using the ray tracing program SHADOW [10,11] which shows the excellent capabilities of the instrument concerning throughput, energy resolution and spot size at the sample using only one additional focusing mirror beyond the exit slit.

A SOFT X-RAY GRATING MONOCHROMATOR FOR UNDULATOR RADIATION

R. Reininger and V. Saile

Hamburger Synchrotronstrahlungslabor HASYLAB at DESY,
Notkestr. 85, 2000 Hamburg 52, Federal Republic of Germany.

One of the new insertion devices to be installed in the expansion of the DORIS storage ring consists of three undulators designed to cover with the first harmonic the photon energy range between 70 and 2000 eV. The concepts for a high resolution and high throughput monochromator that will take full advantage of this powerful new beam line are discussed. The final design is a modified SX-700 type monochromator in which the focusing elliptical mirror is replaced by a spherical one. The aberrations due to the new mirror are minimized by elongating the exit slit arm of the conventional SX-700. The ultimate resolution expected is 0.03 eV at 152 eV and 0.6 eV at 1086 eV with a photon flux up to 5×10^{11} photons/(sec 100 mA) at the sample. The spot size at the sample position is less than 0.4×1.0 mm².

ISSN 0723 - 7979

DESIGN CONSIDERATIONS

The optical design of the conventional SX-700 monochromator has been discussed by Petersen [1-3]. It is in principle an instrument based on a plane grating as the original GLEISPIMO monochromator [12]. If α and β are the angles of incidence and diffraction at the plane grating and if r is the distance between the source and the grating then the virtual monochromatic source will be at a distance

$$r' = -r \left[\frac{\cos \beta}{\cos \alpha} \right]^2 = -rc^2 \quad (1)$$

behind the grating. Wavelength scanning performed by rotating the grating results, therefore, in a virtual monochromatic source at a variable distance. This can be eliminated by keeping the ratio $\cos \beta / \cos \alpha$ constant (fix-focus mode) with the help of a plane pre-mirror as implemented in the SX-700.

The condition $c = \text{const.}$ implies that the pre-mirror has to be rotated as well as translated in order to illuminate the grating at the required angle. A simple mechanical solution, namely, a single rotation around an axis mounted outside the mirror surface [13] was adopted instead by the manufacturer of the SX-700 (C. Zeiss, Oberkochen). The ratio c was chosen by Petersen [2] as 2.25 by considering grating efficiencies in the soft x-ray region.

The focusing of the fixed virtual source into the exit slit is performed in the standard instrument by an elliptical mirror. If r_1 and r_2 are the virtual source-mirror and mirror-slit distance, respectively, then the vertical spot size at the exit slit plane is given by

$$\Delta z' = \Delta z c (r_2 / r_1), \quad (2)$$

where Δz is the vertical source size.

It is well known, that the optimal resolution of a vertically dispersing grating monochromator is determined by the vertical source size. The size and divergence of the electron beam at the position of the XUV undulators for DORIS III were optimized [14] according to this requirement. The actual parameters are summarized in table 1. As seen in the table the vertical source size is relatively large as compared to that found in the newly dedicated low emittance storage rings. This can be compensated for, however, by taking advantage of the large distance we can choose between the source

point and the spherical refocusing mirror (28 m), as shown below.

The replacement of the elliptical focusing mirror by the appropriate spherical one without changing any other parameter in the SX-700 design, besides the grating-source distance, introduces a severe coma aberration. The vertical spot size at the exit slit plane due to this aberration, $\Delta z'_c$, is, in fact, much larger than the corresponding size of the focused source image, $\Delta z'$. For a spherical mirror of length $2w$ and radius

$$R = \frac{2}{\cos \alpha} \left[\frac{1}{r_1} + \frac{1}{r_2} \right]^{-1}, \quad (3)$$

with angle of incidence α , the coma aberration is given by

$$\Delta z'_c = \frac{3}{2} \left[\frac{w^2}{R} \right] \sin \alpha \left[\frac{r_2}{r_1} - 1 \right] \quad (4)$$

By inserting the relevant geometrical parameters in eqs. (3) and (4), namely $r_1 = 2.25^2 \times 28000$ mm, $r_2 = 1000$ mm, $\alpha = 88^\circ$, and $w = 112.5$ mm one obtains $|\Delta z'_c| = 0.33$ mm, which is 26 times larger than the spot size obtained from eq. (2) when taking the FWHM of the vertical source size (table 1).

Two solutions are possible in order to minimize this aberration: to reduce the mirror length at the expense of intensity or to use a mirror with a larger radius and elongating the exit slit arm of the monochromator. The latter does not reduce the throughput of the monochromator. It does, on the other hand, increase $\Delta z'$ but this does not affect the energy resolution since the linear dispersion increases by the same factor. A satisfactory compromise for a reasonable exit slit arm is $r_2 = 6000$ mm at which $\Delta z' (0.076 \text{ mm}) > \Delta z'_c$. The results of the ray tracing calculations described below agree with the analytical solution showing that only the coma aberration is of importance in the present case.

The spot size at the exit slit plane due to surface tangent errors of magnitude σ is given by

$$\Delta z'_s = 2\sigma r_2. \quad (5)$$

The technology for producing the required spherical mirror with $-0.4 < \sigma < 0.4$ arcsec is well established [15]. Eq. 5 yields $\Delta z'_s = 0.048$ mm for such surface tangent errors which translates into a maximum resolution degradation of only 17%.

Figure 1 shows the optical elements of the proposed beamline.

RAY TRACING RESULTS

The parameters of the three undulators [8] are listed in table 2. The divergence of the delivered undulator beam was taken in consideration in the ray tracing calculations. The undulator length, on the other hand, was found to make no significant change in the ray tracing results due to the large source-grating distance. Table 3 gives the parameters of the optical elements relevant to the ray tracing calculations.

The first series of ray tracing calculations were performed in order to determine the minimum mirror-exit slit distance required in order to obtain source size limited resolution. The mirror radius was varied between 56.9 m and 382.27 m. The plane pre-mirror belonging to the monochromator as well as a plane mirror to be installed in the beam line to cut-off the high energy photons were not included in the optical system used in the ray-tracing calculations.

Figure 2a shows the beam spot pattern ($h\nu=1086$ eV) at the exit slit plane for $r_2=6000$ mm ($R=329.9$ m) using the full mirror acceptance (approx. 160×30 mm² at this energy). The results of fig. 2b shows the effect of masking down the mirror to 110mm. The adjacent histograms show that in the dispersing and in the non-dispersing direction the distribution is almost Gaussian. The FWHM in the former direction is 0.087 mm in fig. 1 and 0.077 mm in fig. 2, practically source size limited.

The solid lines in figures 3 and 4 summarize the energy resolution obtained from the linear dispersion and the spot size at the exit slit plane as a function of the mirror-slit distance at 152 eV and 1086 eV, respectively. At 152 eV no photons are lost due to the grating dimensions but only 77% of the monochromatic light is accepted by the mirror. At 1086 eV, 79% of the photons are accepted by the grating and all are refocused by the mirror. As seen in both figures the resolution limit due to the mirror aberrations decreases rapidly with increasing mirror-slit distance without reaching a saturation value. The dashed lines in figures 3 and 4 were deduced from the ray tracing calculations after limiting the mirror length to 110 mm. This

implies rejecting 66% and 35% of the photons at 152 eV and at 1086 eV, respectively. Comparing to the case of the full mirror it is seen that a better resolution is obtained when masking the mirror down as deduced above when considering equation (4). It is also worth noting that in the case of the masked mirror, the source limited resolution is achieved when the exit slit is at 5000 mm from the mirror pole.

The energy resolution derived from ray tracing calculations using a mirror of radius 329.9 m is displayed in Fig. 5 for the case of a zero height exit slit. The minimum spot size obtained from the ray tracing is 75 μ m. Therefore, a smaller exit slit e.g., 20 μ m, should not affect significantly the values presented in the graph. The crosses were obtained without limiting the exposed surface of the focusing mirror. The better resolution, represented by the squares, was obtained by masking down the length of the mirror to 110 mm. The figure also includes the resolution obtained with the conventional optics of the SX-700 monochromators at BESSY. The dashed lines are the results obtained with the SX-700/II installed recently at [5], the resolution in this case is determined by the slope errors of the elliptical mirror. The dotted line shows the performance of the SX-700/I, equipped with the focusing mirror having slope errors of ± 0.9 arcsec [4]. Here the resolution is limited by the source size. The solid line represents the best results achieved with the SX-700/II, obtained after masking down 99% of the elliptical mirror surface [5]. As seen in the figure the replacement of the elliptical mirror by a spherical one, the elongation of the exit slit arm, and the increase of the source-focusing mirror distance improves the performance of the this type of monochromator *even* without reducing the illumination of the spherical mirror surface.

The refocusing of the divergent beam beyond the exit slit can be satisfactorily performed with only one additional mirror. Due to the long exit slit arm and the largest effective height of the mirror (7.85 mm), the maximum vertical divergence is 1.3 mrad. This yields a spot of slightly less than 2 mm in the vertical direction at 1500 mm from the exit slit. It is, therefore sufficient to focus the divergent beam only horizontally. This can be done by using a plane elliptical mirror as the ray tracing results show in Fig. 6a at a photon energy of 1086 eV. As seen in the figure the spot size is less than 0.4×1.8 mm². An improved energy resolution implies, in this design, an improved spot size as well. Limiting the spherical mirror length to 110 mm

means that the divergence in the vertical direction is 0.64 mrad i.e., less than one millimeter at the sample position as demonstrated in Fig. 6b.

The fluxes delivered by the undulator at 152 and 1086 eV are 6×10^{14} and 8×10^{14} photons/(sec \times 100 mA \times 0.1% bandwidth) respectively [8]. Taking into account reflectivity losses due to the 4 mirrors, grating efficiencies of 20% (152 eV) and 5% (1086 eV) [16], an exit slit height of 20 μ m, and the acceptance of the different optical elements one obtains approximately 5×10^{11} and 2.5×10^{11} photons/sec at the sample at the highest resolution for the two photon energies, respectively.

The optical elements will be exposed to considerable heat loads. 1.7 KW will hit the first mirror under the worst conditions namely, use of the low energy undulator with the narrowest gap. Approximately 1.5 KW have to be dissipated in this optical element. The pre-mirror of the monochromator receives 200 Watt, the grating 11 Watt. Therefore, an efficient cooling scheme as well as an appropriate choice of materials like SiC [17] has to be employed for the monochromator.

CONCLUSIONS

We have presented several modifications in the optical concept of the SX-700 monochromator which improve significantly its performance. In particular, the solution presented above is extremely well suited to an undulator beam. The replacement of the focusing elliptical mirror by a spherical one and the extension of the exit slit arm leads to source size limited resolution. The relatively large vertical source size at the position of the undulator is compensated for by the large distance at which the spherical mirror is located and by the demagnification of the plane grating. The choice of a plane grating monochromator without an entrance slit shows that, besides the reflectivity losses and grating efficiency, the undulator beam is efficiently used. The horizontal refocusing beyond the exit slit with a plane elliptical mirror is sufficient to obtain a spot small enough for the experiments planned with this instrument, e.g., high resolution emission spectroscopy in the XUV and photoelectron spectroscopy.

REFERENCES

- [1] H. Petersen.
Optics Comm. 40 (1982) 402 .
- [2] H. Petersen.
Nucl. Instr. & Meth. A246 (1986) 260.
- [3] H. Petersen.
SPIE 733 (1986) 262.
- [4] H. Petersen.
BESSY TB 136/1988.
- [5] D. Arvanitis, H. Rabus, M. Domke, A. Puschmann, G. Comelli, H. Petersen, L. Tröger, T. Lederer, G. Kaindl and K. Baberschke.
Appl. Phys. to be published.
- [6] C.T. Chen and F. Sette.
Rev. Sci. Instr., to be published.
- [7] C.T. Chen.
Nucl. Instr. Meth. A256 (1987) 595.
- [8] J. Pflüger and P. Gürtler.
Nucl. Instr. and Meth., to be published.
- [9] F. Senf, K. Berens, V. Rautenfeldt, S. Cramm, C. Kunz, J. Lamp, V. Saile, J. Schmidt-May, and J. Voss.
Nucl. Instr. & Meth. A246 (1986) 314.
- [10] B. Lal and F. Cerrina.
Nucl. Instr. & Meth. A246 (1986) 337.
- [11] B. Lal, K. Chapman, and F. Cerrina.
Nucl. Instr. & Meth. A266 (1988) 544.
- [12] H. Dietrich and C. Kunz

Rev. Sci. Instr. 43 (1972) 434.

[13] F. Riemer and R. Torge.

Nucl. Instr. & Methods 208 (1983) 313 .

[14] W. Brefeld, H. Neemann, and J. Roßbach.

European Particle Accelerator Conference, ed. S. Tazzari, Rome, (1988),
p. 389.

[15] W. Hasselmann, C. Zeiss (Oberkochen), private communication.

[16] W. Jark.

Nucl. Instr. & Meth. A268 (1988) 414.

[17] S. Mourikis, W. Jark, E.E. Koch, and V. Saile.

Rev. Sci. Instr. 60 (1989) 1474.

Table 1

Electron optics parameters

Electron energy	4.5 Gev
Electron current	100 mA
σ_x	3.1 mm
σ'_x	0.13 mrad
σ_z	0.34 mm
σ'_z	0.039 mrad

Table 2

Undulator parameters, K is the wiggler parameter.

Energy (eV)	Period (cm)	Number	Length (m)	Field (T)	K	Total Power (KW/100 mA)
50-400	11.91	33	4.0	0.71	7.91	2.54
200-1000	8.83	45	4.0	0.54	4.45	1.47
800-2000	6.58	60	4.0	0.38	2.30	0.71

Table 3

Optical components used in the ray tracing calculations.

(The length units are in mm, angles are in degrees, the distance is relative to the source point, and the groove density in gr/mm)

	Dimensions	Distance	Incidence angle	Groove Density
Grating	110x30	27350	variable	1220 gr/mm
Spherical mirror	225x30	28000	88	
Plane elliptical mirror	600x30	34500	88	
Sample position		35500		

FIGURE CAPTIONS

Figure 1.

Optical layout of the beamline.

Figure 2.

Beam spot pattern ($h\nu=1086$ eV) at the exit slit plane for $r_2=6000$ mm ($R=329.9$ m). x and z are the non-dispersing and dispersing directions, respectively. a) Full mirror acceptance (160×30 mm² at this energy) . b) Active surface of the mirror, 110×30 mm². The adjacent histograms show the number of rays as a function of the x and z coordinates.

Figure 3.

Energy resolution as a function of the mirror-slit distance for $h\nu=152$ eV. The mirror radius varies between 56.9 and 382.27 m.

Figure 4.

As in fig. 3 but for $h\nu=1086$ eV.

Figure 5.

Energy resolution as a function of the photon energy. Symbols: present calculations for a mirror of radius 329.9 m. + full mirror illumination; □, only 110 mm of the mirror length are used. Dotted line, SX-700/I with focusing mirror having slope errors of ± 0.9 arcsec (from Ref [4]). Broken and solid lines; SX-700/II with full mirror illumination and after masking down 99% of the elliptical mirror surface, respectively (from Ref. [5]).

Figure 6.

a) and b) As in Fig. 2 but at the sample plane.

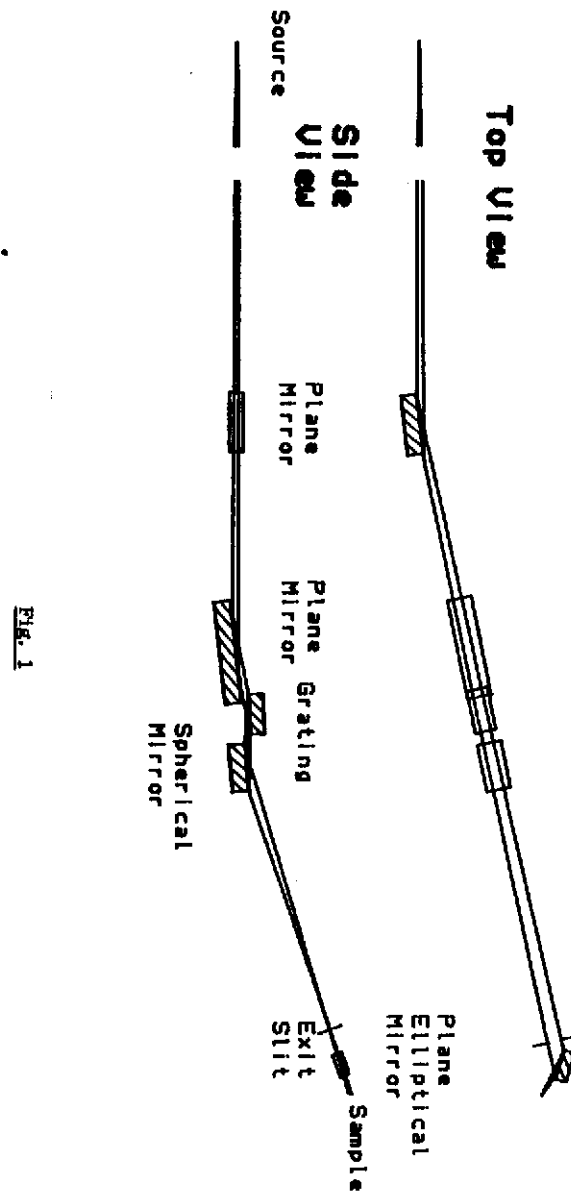


Fig. 1

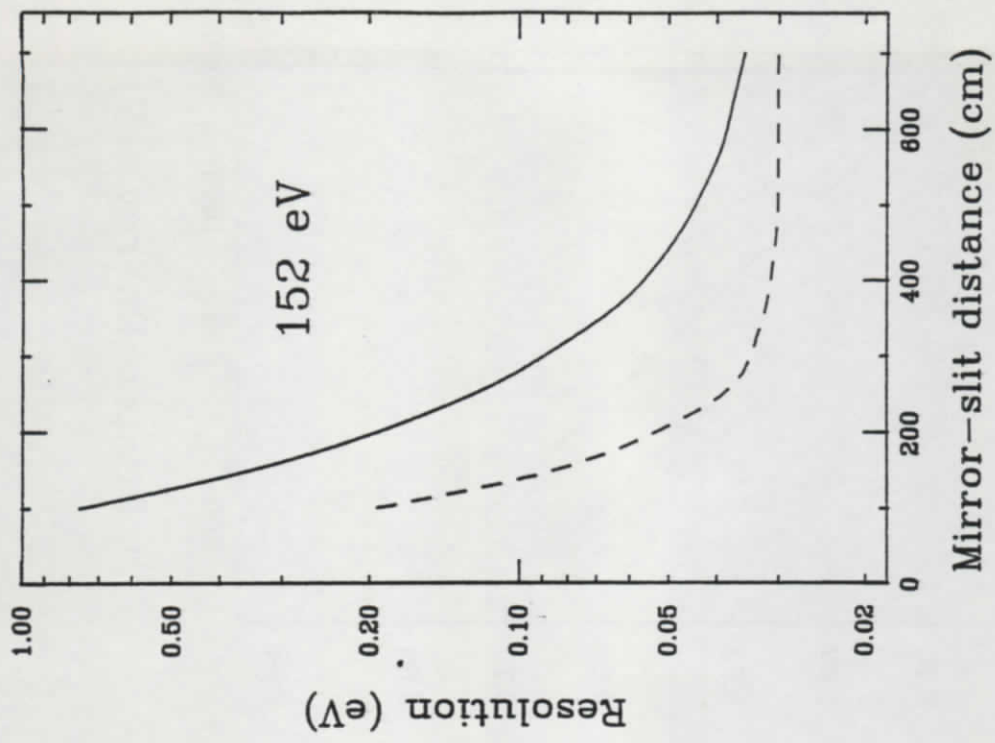


Fig. 3

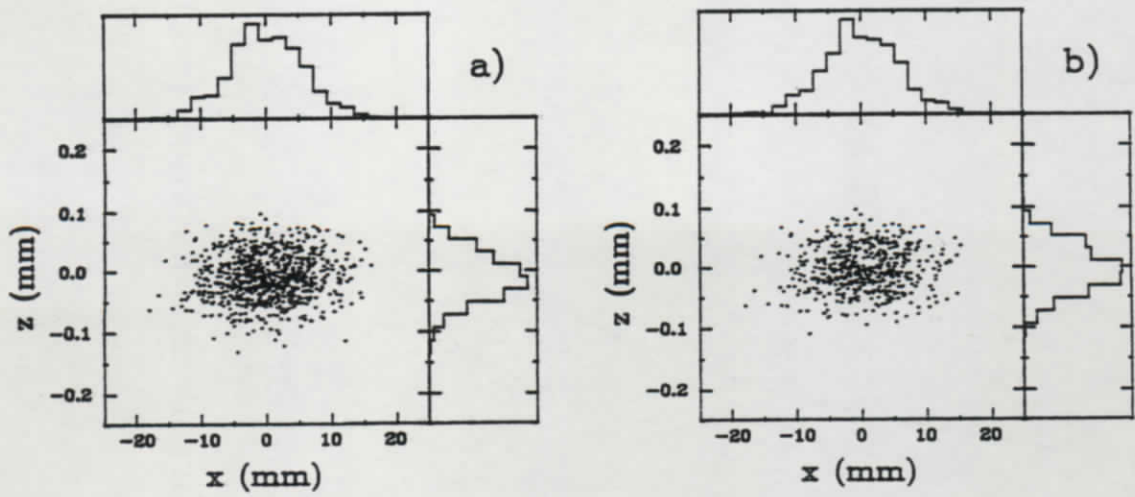


Fig. 2

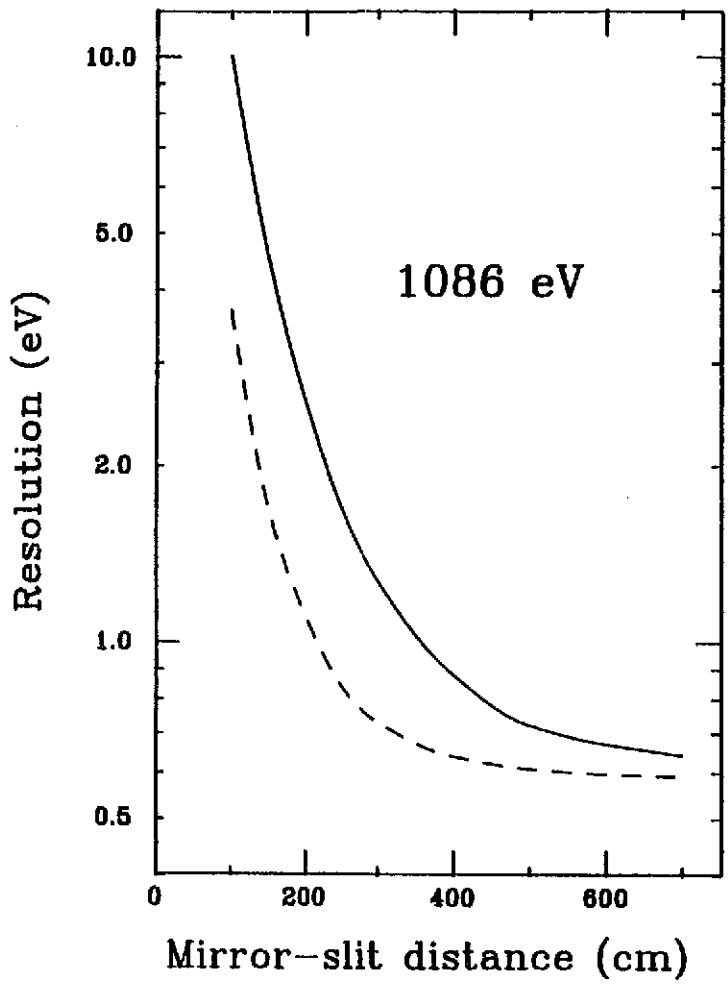


Fig. 4

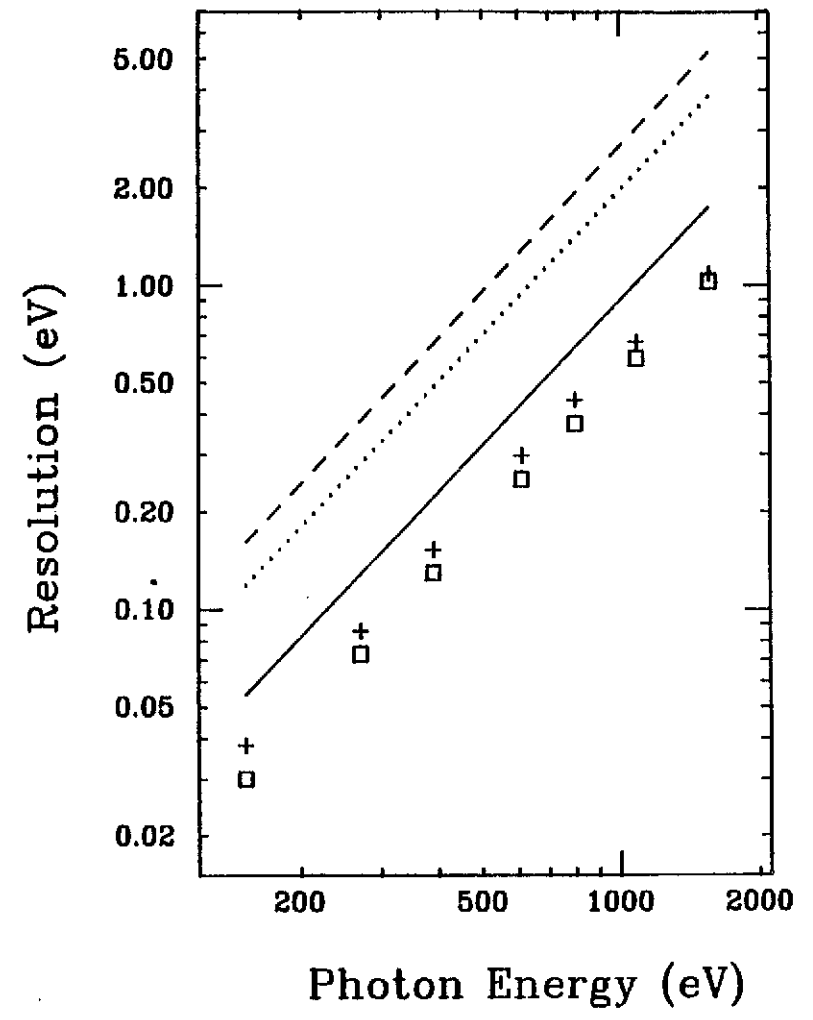


Fig. 5

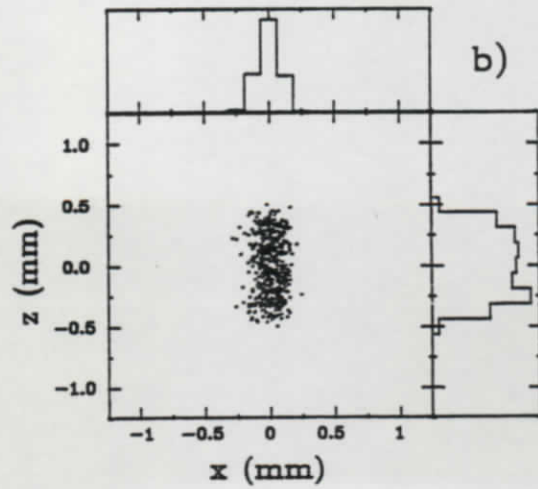
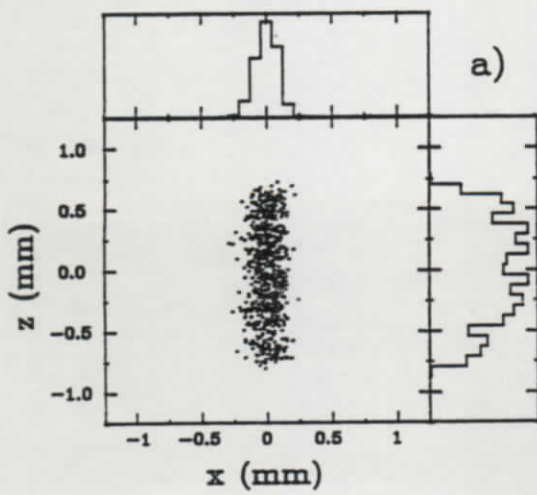


Fig. 6

